ISSN 2658-3518

LIMNOLOGY & FRESHWATER BIOLOGY

2021, № 3

> abiotic and biotic water components;
> ecosystem-level studies;
> systematics and aquatic ecology;
> paleolimnology and environmental histories;
> laboratory experiments and modeling

Limnology and Freshwater Biology 2021 (3): 1143-1146 DOI:10.31951/2658-3518-2021-A-3-1143

Short communication

ISSN 2658-3518
LIMNOLOGY FRESHWATER BIOLOGY
www.limnolfwbiol.com

Identification of Baikal phytoplankton inferred from computer vision methods and machine learning

Lysenko A.V.[1,2]*, Oznobikhin M.S.[1,2], Kireev E.A.[1,2], Dubrova K.S.[1], Vorobyeva S.S.[1]

[1] *Limnological Institute, Siberian Branch of the Russian Academy of Sciences, Ulan-Batorskaya str., 3, Irkutsk, 664033, Russia*
[2] *Institute of Mathematics and Information Technologies, Irkutsk State University, Gagarina str., 20, Irkutsk, 664003, Russia*

ABSTRACT. This study discusses the problem of phytoplankton classification using computer vision methods and convolutional neural networks. We created a system for automatic object recognition consisting of two parts: analysis and primary processing of phytoplankton images and development of the neural network based on the obtained information about the images. We developed software that can detect particular objects in images from a light microscope. We trained a convolutional neural network in transfer learning and determined optimal parameters of this neural network and the optimal size of using dataset. To increase accuracy for these groups of classes, we created three neural networks with the same structure. The obtained accuracy in the classification of Baikal phytoplankton by these neural networks was up to 80%.

Keywords: phytoplankton classification, machine learning, transfer learning, image processing, computer vision

1. Introduction

In the modern world, machine-learning methods are becoming increasingly applicable in different fields of science. For example, they are used in the sequence data mining of DNA (Yang et al., 2020). Computer vision methods and neural networks are widely used in biology for object recognition (Majaj and Pelli, 2018; Sánchez et al., 2019). In biology, recognition of objects in an image provides automatization of statistical analysis of organisms, biomass counting, etc. Usually, biologists analyze these images manually, whereas using special software will help to classify objects faster. Additionally, a software interface will allow the user to use the program for one specific image or for a set of images. It makes the program more visually clear for any user.

One of the most widely used image classification methods is convolutional neural networks. Convolutional neural networks are a very large class of architectures, the main idea of which is to alternate convolutional layers and pooling layers. The structure of this network is unidirectional and multilayered. A convolutional neural network consists of an input layer, hidden layers and an output layer. These hidden layers usually consist of convolutional layers, pooling layers, fully connected layers, and normalization layers (Hussain et al., 2018). Convolution neural networks have applications (Yamashita et al., 2018) in image classification, image segmentation, object detection, image and video recognition as well as in natural language processing. Neural networks that are used for classification usually contain the same number of output neurons in the last layer as the number of classes. This output vector is a set of probabilities of images belonging to each class. The highest probability value corresponds to the neural network prediction.

Transfer learning is often used to improve the accuracy of the prediction of the neural network. Transfer learning is a machine learning technique that focuses on using the experience gained from solving one problem to solve another similar problem. At first, the neural network is trained on a large amount of data, then on the purpose dataset. This method is often used when a purpose dataset is smaller than the original dataset used to train the pre-trained model (Larsen-Freeman, 2013). Also, transfer learning is applied in such types of biology tasks as plant image classification (Tapas, 2016).

There are many computer vision methods for image segmentation and object detection. It can be also done using neural networks. The application of computer vision methods for segmentation requires converting an image to grayscale and then binarizing it. One of the most popular binarization techniques is Otsu's method. This algorithm returns a single intensity threshold that separates pixels into two classes, foreground and background (Otsu, 1979). The Otsu's method also

*Corresponding author.
E-mail address: allessouth@gmail.com (A.V. Lysenko)

Received: June 28, 2021; ***Accepted:*** July 12, 2021;
Available online: September 2, 2021

has an improved version to support multiple image levels, which is called the multi-Otsu method (Liao et al., 2001). Another popular binarization technique is Canny Edge Detection (1986). This technique allows the detection of a wide range of edges in images. For our dataset, Otsu's method demonstrated the best results. After binarization of the image, the pixels that belong to the regions of interest take the value of 1.

Data augmentation is a technique for creating additional training data from existing data. It acts as a regularizer and helps reduce overfitting when training a machine learning model (Shorten and Khoshgoftaar, 2019). To achieve good results, neural networks must be trained on a large amount of data. Therefore, if the original dataset contains a limited number of images, it is necessary to perform data augmentation to improve the results of the work of the neural network. There are many techniques to do data augmentation such as the popular horizontal flipping, vertical flipping, random crop, random rotation, etcetera (Shorten and Khoshgoftaar, 2019). Also, there are color augmentation techniques, and the most popular of them are histogram equalization, white-balancing, sharpening, blurring, and enhancing contrast or brightness (Galdran et al., 2019). Several of these techniques can be combined. Implemented augmentation techniques increase the original dataset by a factor of 10.

In our study, we try to connect computer vision methods and machine learning for the classification of phytoplankton in Lake Baikal.

2. Materials and methods

Phytoplankton samples were collected from the shallow zone at the Listvyanka settlement (southern basin of Lake Baikal) 51.868022 N, 104.82959 E from February to May 2021. This area has no continuous ice cover during winter. The samples were fixed with the Utermöhl solution and concentrated by sedimentation. The concentrate was placed into a 0.1 mL cell and examined under an Amplival (Carl Zeiss, Germany) microscope at 640x magnification.

The original dataset consisted of 2705 images with dimensions of 3488x2616, each of which might contain several instances of each class of recognizable objects. 4622 original phytoplankton images were obtained by manual segmentation. Our neural network was constructed based on the phytoplankton taxa *Cyclotella minuta* Antipova (162 images), *Aulacoseira baicalensis* (K. Meyer) Simonsen (295 images), *Synedra acus* subsp. *radians* (Kütz.) Skabitsch (213 images), *Cryptomonas* sp. (527 images), *Rhodomonas pusilla* (Bachm.) Javorn. (155 images), *Dynobrion cylindricum* Imhof (411 images), *Gyrodinium helveticum* (Penard) (226 images), *Peridinium baicalense* Kiselev et Cvetkov (314 images), *Gymnodinium baicalense* (197 images), and *Koliella longiseta* (Vischer) Hindak (205 images).

The Watershed algorithm was applied to image segmentation. The input image was blurred with mean shift filtering and converted to grayscale. The resulting image was binarized with Otsu's method. Then, the distance to the closest zero pixels for each pixel of the source image was calculated. After distance calculating, we found local maxima and implemented the Watershed algorithm. The result of applying this algorithm is a matrix of labels that can be converted into an image. Segmented objects have different numeric labels, and it allows selecting them according to these numerical labels.

We used a pre-trained Xception neural network (Chollet, 2017) as the initial network and created a 'target' neural network using transfer learning (Pratt and Jennings, 1996) technology, in which two dense layers were used, including 1024 and 512 neurons. We used the following parameters of the neural network: the rectified linear unit (ReLU) activation function, dropout of 30% (to avoid retraining of the neural network) and the output layer, with softmax activation function. To train the neural network, the following datasets were used for each of the 10 species: 184 images for training and 30 images for validation. Learning took place for 100 epochs with the stochastic gradient descent (SGD) optimization function and the learning rate parameter equal to 0.005.

3. Results and discussion

The analyzed phytoplankton taxa were different in i) outlet contours from oval to rectangular (Fig. 1) and ii) grouping of objects from single to mass clusters (Fig. 2). As a result, the program detects single objects in the images with an accuracy of 90%. In images with noisy regions or other objects (such as incomplete parts of objects), the accuracy decreased to 72%. In the case of objects intersection when many objects have a common border the accuracy reaches 59%. For a sample of images of each type, the accuracy was 62% (Fig. 2).

The trained neural network most accurately identifies *A. baicalensis*, *Cryptomonas* sp., *C. minuta, D. cylindricum*, *K.longiseta*, *P. baicalense*, and *S. acus* with an accuracy > 80% (Table). The most mistakes concerned the identification of *Rh. pusilla* with an accuracy of 48% where 48% of images were regarded as *Cryptomonas* sp. It was unexpected because *Cryptomonas* sp. was detected with high reliability (Table) and confused only with *Rh. pusilla* in 11% cases. For this reason, the special train neural network was formed for only these two species. The accuracy of this neural network is 96% for the recognition of *Cryptomonas* sp. and 77% for *Rh. pusilla*. Moreover, other spatial network was formed for the assemblage of *G. helveticum*, *P. baicalense* and *G. baicalense*. The accuracy of this neural network was 90% for *G. helveticum*, 88% for *G. baicalense*. and 96% for *P. baicalense*. The architecture of these neural networks was the same; the differences were only in the number of neurons in the output layer.

At present, the phytoplankton assemblage of Lake Baikal is characterized by 70 taxa and their species. The amount of phytoplankton changed from 0.015 to 136 million cells L^{-1} with biomass of 0.004-2.13 g m^{-3}. Diatoms (20 taxa) were represented by *A. baicalensis*, *A. islandica*, *C.minuta*, *C. baicalensis*, *Nitzschia graciliformis*, *S.acus*, and *Stephanodiscus meyeri*. *Gyrodinium*

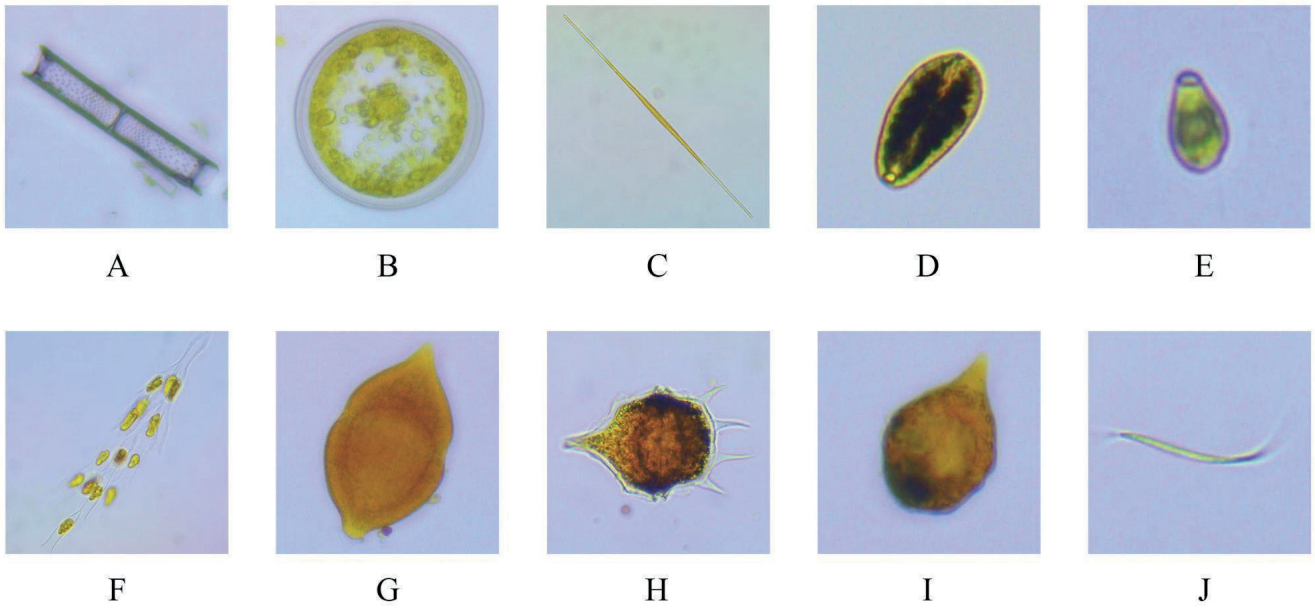

Fig.1. Sample images of phytoplankton taxa that can be recognized by software in this study (A - *Aulacoseira baicalensis,* B - *Cyclotella minuta*, C - *Synedra acus*, D - *Cryptomonas*, E - *Rhodomonas pusilla*, F - *Dynobrion cylindricum*, G - *Gyrodinium helveticum*, H - *Peridinium baicalense*, I - *Gymnodinium baicalense*, and J - *Koliella longiseta*).

helveticum, *G. baicalense*, *P.baicalense* and *Glenodinium* sp. predominate in Dinophyta. *Rhodomonas pusilla* (up to 6064 thousand cells L^{-1}) dominated Cryptophyta. Chrysophyta were formed by *Chrysochromulina parva* (up to 6439 thousand cells L-1) and *D.cylindricum* (up to 192 thousand cells L-1). Chlorophyta was represented by *Monoraphidium contortum*, *M. arcuatum*, *K. longiseta*, and *Chlamydomonas* sp (Vorobyeva, 2018; Bondarenko et al., 2020). Hence, the constructed three networks can help to identify the main taxon of the Baikal phytoplankton with high accuracy.

4. Conclusions

In this study, we tested the neural networks for the identification of the Baikal phytoplankton assemblage. One neural network did not define accurately large data set of species of Diatoms, Dinophyta, Cryptophyta, Chrysophyta, and Chlorophyta in the Baikal phytoplankton. We constructed three networks for i) *A. baicalensis*, *C. minuta, D. cylindricum*, *K.longiseta*, *P. baicalense*, *S. acus*; ii) *Cryptomonas* sp. and *Rh. usilla*; iii) *G. helveticum*, *P. baicalense* and *G. baicalense.* The accuracy of these neural networks was >80%. The software developed for object detection allows segmenting of many objects in images. This software can detect isolated objects with high accuracy. This is more difficult to allocate objects in noisy images than to allocate single objects in non-noisy images. In the future, it will be necessary to supplement the dataset with rare species because the number of images, on which the neural network is trained, in some species is more than 50% of the number of images of this species in the general dataset that we tested. Therefore, the results are undoubtedly less reliable.

Acknowledgments

The authors thank A.S. Kazimirov from Institute of Mathematics and Information Technologies, Irkutsk State University for theoretical advice.

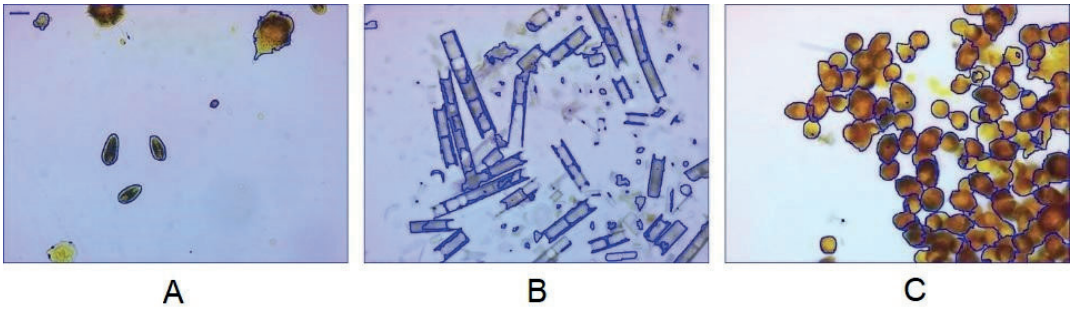

Fig.2. Sample images of phytoplankton clusters with contour detection examples (A - isolated objects, B - objects in noisy image, C - intersecting objects in image without noise).

Table. Recognition results.

actual class in test dataset	distribution of predictions, percent									
	A. baicalensis	*Cryptomonas* sp.	*C. minuta*	*D. cylindricum*	*G. helveticum*	*G. baicalense*	*K. longiseta*	*P. baicalense*	*Rh. pusilla*	*S. acus*
A. baicalensis	**94**	0	0	0	0	0	0	0	0	**5**
Cryptomonas sp.	0	**89**	0	0	0	0	0	0	**11**	0
C. minuta	0	0	**98**	0	0	1	0	0	0	0
D. cylindricum	0	0	0	**100**	0	0	0	0	0	0
G. helveticum	0	4	0	0	64	**13**	0	**17**	1	0
G. baicalense.	0	**5**	0	0	**9**	68	0	**17**	1	0
K. longiseta	0	0	0	1	0	0	**95**	0	0	3
P. baicalense	0	1	0	1	**3**	**6**	0	**89**	0	0
Rh. pusilla	0	**48**	1	0	0	0	0	1	48	0
S. acus	**5**	0	0	2	0	0	**8**	0	0	**84**

In this table, the rows correspond to the actual value, and the columns - to the predicted value; when they intersect, the prediction is considered correct.

Conflict of interests

The authors declare no conflicts of interest.

References

Canny J. 1986. A computational approach to edge detection. IEEE Transactions on Pattern Analysis and Machine Intelligence 8(6): 679-698. DOI: 10.1109/TPAMI.1986.4767851

Chollet F. 2017. Xception: deep learning with depthwise separable convolutions. In: IEEE Conference on Computer Vision and Pattern Recognition. DOI: 10.1109/CVPR.2017.195

Galdran A., Alvarez-Gila A., Meyer M.I. et al. 2017. Data-driven color augmentation techniques for deep skin image analysis. arXiv:1703.03702v1.

Hussain M., Bird J.J., Faria D.R. 2018. A study on CNN transfer learning for image classification. In: 18th Annual UK Workshop on Computational Intelligence. DOI: 10.1007/978-3-319-97982-3_16

Larsen-Freeman D. 2013. Transfer of learning transformed. Language Learning 63(s1). DOI: 10.1111/j.1467-9922.2012.00740.x

Liao P.-S., Chen T.-S., Chung P.-C. 2001. A fast algorithm for multilevel thresholding. Journal of Information Science and Engineering 17(5): 713-727. DOI: 10.6688/JISE.2001.17.5.1

Otsu N. 1979. A threshold selection method from gray-level histograms. IEEE Transactions on Systems, Man, and Cybernetics 9(1): 62-66. DOI: 10.1109/TSMC.1979.4310076

Pratt L., Jennings B. 1996. A survey of transfer between connectionist networks. Connection Science 8(2): 163-184. DOI: 10.1080/095400996116866

Sánchez C., Cristóbal G., Bueno G. 2019. Diatom identification including life cycle stages through morphological and texture descriptors. PeerJ 7. DOI: 10.7717/peerj.6770

Shorten C., Khoshgoftaar T.M. 2019. A survey on image data augmentation for deep learning. Journal of Big Data 6(1). DOI: 10.1186/s40537-019-0197-0

Tapas A. 2016. Transfer learning for image classification and plant phenotyping. In: Second International Conference on Electronics, Communication and Aerospace Technology. DOI: 10.1109/ICECA.2018.8474802

Vorobyeva S.S. 2018. Phytoplankton assemblages of the Southern Baikal in 1990-1995 and 2016-2018. Limnology and Freshwater Biology. 1(2): 141-143. DOI: 10.31951/2658-3518-2018-A-2-141

Bondarenko N.A., Vorobyova S.S., Zhuchenko N.A. et al. 2020. Current state of phytoplankton in the littoral area of Lake Baikal, spring 2017. Journal of Great Lakes Research 46(1): 17-28. DOI: 10.1016/j.jglr.2019.10.001

Yang A., Zhang W., Wang J. et al. 2020. Review on the application of machine learning algorithms in the sequence data mining of DNA. Frontiers in Bioengineering and Biotechnology 8. DOI: 10.3389/fbioe.2020.01032

Yamashita R., Nishio M., Do R.K.G. et al. 2018. Convolutional neural networks: an overview and application in radiology. Insights into Imaging 9(4). DOI: 10.1007/s13244-018-0639-9

Majaj N.J., Pelli D.G. 2018. Deep learning - using machine learning to study biological vision. Journal of Vision 18(13):2: 1-13. DOI: 10.1167/18.13.2

Limnology and Freshwater Biology 2021 (3): 1147-1151 DOI:10.31951/2658-3518-2021-A-3-1147

Short communication

ISSN 2658-3518
LIMNOLOGY FRESHWATER BIOLOGY
www.limnolfwbiol.com

Optical characteristics of water at the mouth of the Ob River

Akulova O.B.*, Bukaty V.I., Kirillov V.V.

Institute for Water and Environmental Problems, Siberian Branch of the Russian Academy of Sciences, 1, Molodezhnaya St., 656038 Barnaul, Russia

ABSTRACT. As a result of the field studies (August 25 – September 1, 2020), new data were obtained on the optical characteristics of water at the Ob River mouth near the Salemal village (Yamal region, Yamal-Nenets Autonomous Okrug) during the lowest water level and the maximum development of hydrobiocenoses. We calculated the light attenuation coefficient $\varepsilon(\lambda)$ in the spectral range from 400 to 800 nm, which varied from 1.5 to 21.5 m^{-1} during the study period, and the light absorption by yellow substance $\kappa_{ys}(\lambda)$ from 0.1 to 12.2 m^{-1}. Concentrations of yellow substance C_{ys} and chlorophyll *a Chl* were determined. For instance, chlorophyll *a* concentrations in water samples taken at different stations of the Ob River ranged from 12.5 to 22.7 $mg \cdot m^{-3}$. The maximum content of chlorophyll *a* in our case was recorded at a depth of 14 m (station 5.3), which was 22.7 $mg \cdot m^{-3}$. The yellow substance concentration determined optically by the calculated yellow substance light absorption coefficient at wavelength $\lambda = 450$ nm ranged within 18.8 and 26.9 $g \cdot m^{-3}$ with an average value of 22.1 $g \cdot m^{-3}$. The average value of $\kappa_{ys}(\lambda)$ at $\lambda = 450$ nm over the study period was 4.7 m^{-1}.

Keywords: spectral transparency of water, coefficients of light attenuation and absorption, colored dissolved organic matters, yellow substance, chlorophyll *a*, suspension, physical model, the Ob River

1. Introduction

Hydrooptical monitoring of natural water bodies widely uses measurements of spectral light attenuation coefficients $\varepsilon(\lambda)$, which are important optical characteristics containing information about the state of the aquatic environment. Their value depends on the content of optically active components in water, namely suspended solids, chlorophyll, yellow substance, and pure water (Kopelevich, 1983; Hong et al., 2004; Churilova et al., 2008; 2018; Man'kovsky, 2011; Levin, 2014; Efimova et al., 2016). Many tasks related to the assessment of the state of natural water require knowledge of the contribution of these components to $\varepsilon(\lambda)$ at different parts of the spectrum. The universality of the physical model of light attenuation in aquatic media used in this work allows to us expressly determine in real time the physical parameters of individual water components, in particular, the concentration and size of suspended solids particles, chlorophyll and yellow substance as well as to assess the trophicity of water bodies by their optical properties.

This work is devoted to the study of the optical characteristics of water at the control site "Salemal" in the last control section of the Ob River before the delta during the period from August 25 to September 1, 2020.

2. Materials and methods

The object of the study is the mouth area of the Ob River, a compound natural complex located at the confluence of the Ob, Nadym, Pur, and Taz rivers into the Kara Sea, within which specific estuarine processes occur due to the interaction and mixing of river and sea waters as well as to delta formation processes. It includes the estuaries of the Ob, Nadym and Taz rivers and the vast estuarial coastal area: Ob Bay and Taz Bay. The studies were carried out during the period of the lowest water level (according to the long-term average data of the State Committee for Hydrometeorology) and the maximum development of the river hydrobiocenoses (Yermolaeva et al., 2021). This combination of biotic and abiotic characteristics of the ecosystem determines the special ratio of their contribution to the optical properties of water.

The work was based on the results of treatment and analysis of 14 water samples taken at different depths of the Ob River study site. Observations were carried out at the mouth of the Ob River near the Salemal village, Yamal region, YNAO, from August 25 to September 1, 2020. Table shows the station numbers and sampling depths as well as their coordinates.

Light attenuation $\varepsilon(\lambda)$ and absorption by the yellow substance $\kappa_{ys}(\lambda)$ were measured in the

*Corresponding author.
E-mail address: akulova8282@mail.ru (O.B. Akulova)

Received: July 26, 2021; ***Accepted:*** September 9, 2021;
Available online: October 05, 2021

laboratory in the wavelength range from 400 to 800 nm with an interval of 30 nm using a PE-5400UF single-beam spectrophotometer operating in the mode of measuring the spectral transparency (transmittance) of water. To determine the spectral transparency of water, we used a spectrophotometric method based on the principle of measuring the ratio of intensities of two light fluxes passing through the studied and reference media. A total of 336 measurements of spectral water transparency were carried out. Highly purified distilled water was used as the reference medium, a control sample, in relation to which the measurements were made. The light absorption by yellow substance $\kappa_{ys}(\lambda)$ was defined after measuring the spectral transparency of the water purified from aqueous suspension and chlorophyll *a* through "Vladipor" membranes of MFAS-OS-1 type with a pore diameter of 0.22 μm. The values of $\varepsilon(\lambda)$ and $\kappa_{ys}(\lambda)$ (at the natural logarithmic base) were calculated by the formula, according to expression (1), excluding the spectral coefficient of pure water $\kappa_{pw}(\lambda)$.

$$\varepsilon(\lambda) = \left(\frac{1}{L}\right) \cdot \ln\left(\frac{1}{T(\lambda)}\right), \quad (1)$$

where L is the cuvette length; $T(\lambda) = I(\lambda) / I_0(\lambda)$ – the transparency (transmittance) in relative units; $I(\lambda)$, $I_0(\lambda)$ – the intensity of transmitted and incident light, respectively, and λ – the wavelength of light.

The absolute error of $\varepsilon(\lambda)$ and $\kappa_{ys}(\lambda)$ is induced by the spectrophotometer error during transmittance measurement ($\Delta T = 0.5\%$) and the error measurement of a cuvette length. In the experiment, we used cuvettes $L = 50$ mm long. The maximum absolute error in defining $\varepsilon(\lambda)$ and $\kappa_{ys}(\lambda)$ amounted to 0.1 m^{-1}.

The concentration of yellow substance C_{ys} was determined from the expression given in (Man'kovsky, 2015)

$$C_{ys} = \kappa_{ys}(450) / \kappa_{sp.ys}(450), \quad (2)$$

where $\kappa_{sp.ys}(\lambda)$ is specific light absorption by yellow substance (Nyquist, 1979) at $\lambda = 450$ nm. The effective value $\kappa_{ys}(\lambda)$ in formula (2) is also given by a similar calculation as above by summing $\kappa_{pw}(\lambda)$.

The nature of light absorption by yellow substance is due to electronic transitions in the molecules of organic compounds (Shifrin, 1983). The spectral dependence of light absorption by yellow substance $\kappa_{ys}(\lambda)$ is described by the exponential law (Kopelevich, 1983)

$$\kappa_{ys}(\lambda) = e^{-\mu \cdot \lambda}, \quad (3)$$

where μ is the coefficient characterizing the slope of the spectral absorption curve, the value of which is not constant for different water bodies.

The relative spectral contribution of optically active components of water (suspension, yellow substance, chlorophyll, and pure water) to $\varepsilon(\lambda)$ was calculated using a modified semi-empirical spectral model of light attenuation (Akulova, 2015), which was first proposed by O.V. Kopelevich (Kopelevich, 1983). It looks as

$$\varepsilon(\lambda) = \kappa_{chl}(\lambda) + \kappa_{ys}(\lambda) + \sigma_{mol}(\lambda) + \sigma_s(\lambda) + \kappa_{pw}(\lambda), \quad (4)$$

where $\kappa_{chl}(\lambda)$ and $\kappa_{ys}(\lambda)$ are spectral absorptions by chlorophyll and yellow substance, respectively; $\sigma_{mol}(\lambda)$ is spectral scattering by pure water; $\sigma_s(\lambda)$ is spectral dispersion by suspension, and $\kappa_{pw}(\lambda)$ is spectral absorption by pure water. The calculated attenuation, according to the formula (1), does not contain data on the attenuation by pure water $\varepsilon_{pw}(\lambda) = \kappa_{pw}(\lambda) + \sigma_{mol}(\lambda)$. Thus, in (4), the values of $\varepsilon(\lambda)$ obtained due to spectrophotometer measurements should be summed up with the values of $\varepsilon_{pw}(\lambda)$ taken from the reference data (Smith and Baker, 1981; Pope and Fry, 1997). That was done in our research.

The chlorophyll absorption was calculated using the formula

$$\kappa_{chl}(\lambda) = \kappa_{sp.chl}(\lambda) \cdot C_{chl}, \quad (5)$$

where C_{chl} is the concentration of chlorophyll *a*, $mg \cdot m^{-3}$, and $\kappa_{sp.chl}(\lambda)$ is the specific chlorophyll absorption, $m^2 \cdot mg^{-1}$ (Kopelevich, 1983). To calculate $\kappa_{pw}(\lambda)$, we used the tabular data from (Smith and Baker, 1981; Pope and Fry, 1997), and for $\sigma_{mol}(\lambda)$ – (Smith and Baker, 1981).

As suggested in expression (4), spectral light attenuation is described via a three-parameter model. In contrast to the previous studies, where parameter $\sigma_s(\lambda)$ is determined experimentally, and $\kappa_{ys}(\lambda)$ is the difference between the measured $\varepsilon(\lambda)$ and the sum of other parameters, we propose an alternative approach. Since parameter $\kappa_{ys}(\lambda)$ was determined experimentally, spectral scattering by suspension $\sigma_s(\lambda)$ can be found from the expression (4) with the following formula:

$$\sigma_s(\lambda) = \varepsilon(\lambda) - \left[\kappa_{chl}(\lambda) + \kappa_{ys}(\lambda) + \sigma_{mol}(\lambda) + \kappa_{pw}(\lambda)\right]. \quad (6)$$

The concentration of chlorophyll *a* was found by a standard spectrophotometric method according to GOST 17.1.4.02-90. Relative transparency of Z was measured using a Secchi disk.

3. Results and discussion

During the study period, the spectral light attenuation, $\varepsilon(\lambda)$, within 400–800 nm in water samples taken at different depths of the Ob River at the site near the village of Salemal during the lowest water levels varied from 1.5 to 21.5 m^{-1}; the light absorption by yellow substance $\kappa_{ys}(\lambda)$ ranged from 0.1 to 12.2 m^{-1}. The average value of κ_{ys} at $\lambda = 450$ nm over the study period was 4.7 m^{-1}. The concentration of yellow substance, C_{ys}, in water samples taken at 14 stations of the Ob River was in the range from 18.8 to 26.9 $g \cdot m^{-3}$ with an average of 22.1 $g \cdot m^{-3}$ (Table).

Relative transparency measured by Secchi disk at different stations was ~ 1.0 m.

For example, Figure shows spectral curves of individual optical characteristics obtained for the surface layer of the Ob River station 1.1 (sample taken on August 27, 2020).

The same methodological approach based on the physical model of light attenuation in the aquatic environment was previously used to study the seasonal dynamics and spatial distribution of optical characteristics of river waters in Europe (Pawlak et al., 2003), the USA (Julian et al., 2008) and South America (Lobo et al., 2017).

Based on the results of two field trips to the Tapajós River Basin during the period of the highest water level, data on the total light attenuation, $\varepsilon(\lambda)$, in the range from 390 to 750 nm were obtained (Lobo et al., 2017). We defined $\varepsilon(\lambda)$ as the sum of light absorption, $\kappa(\lambda)$, and scattering, $\sigma(\lambda)$, by aquatic environment. In turn, the total absorption coefficient, $\kappa(\lambda)$, was determined as the sum of absorption coefficients by pure water, $\kappa_{pw}(\lambda)$, dispersed material, $\kappa_s(\lambda)$, and colored dissolved organic matter (yellow substance), $\kappa_{ys}(\lambda)$. Similarly, the total scattering coefficient was determined as the sum of $\sigma_{mol}(\lambda)$ and $\sigma_s(\lambda)$, assuming that the total scattering is negligible due to the yellow substance light scattering coefficient, $\sigma_{ys}(\lambda)$. Consequently, we found that the values of $\kappa_{ys}(\lambda)$ for the presented five classes of water were in the narrow range from 2.0 to 3.5 m^{-1} at $\lambda = 440$ nm. The values of light absorption by the yellow substance obtained for the Ob River at $\lambda = 450$ nm varied within a close range from 4.0 to 5.7 m^{-1}.

Pawlak et al. (2003) presented seasonal variations of light attenuation, $\varepsilon(\lambda)$, in the 300–800 nm range at different sites of the Oder River in the Szczecin region. For example, for the first measurement site at a wavelength of about $\lambda = 300$ nm, the value of $\varepsilon(\lambda)$ was up to 45.8 m^{-1} (fall), 30.32 m^{-1} (winter) and 54.16 m^{-1} (spring). At $\lambda = 750$ nm, the value of $\varepsilon(\lambda)$ was 6.78 m^{-1} (fall), 1.99 m^{-1} (winter) and 7.38 m^{-1} (spring).

Julian et al. (2008) also presented the data on

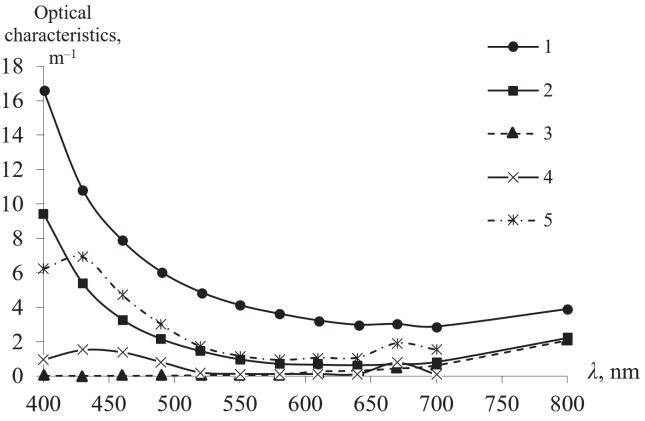

Fig. Spectral dependencies of optical characteristics
1 – light attenuation coefficient $\varepsilon(\lambda)$; 2 – light absorption by yellow substance $\kappa_{ys}(\lambda)$; 3 – attenuation by pure water $\varepsilon_{pw}(\lambda)$; 4 – light absorption by chlorophyll *a* $\kappa_{chl}(\lambda)$; 5 – spectral dispersion by suspension $\sigma_s(\lambda)$

the total light attenuation $\varepsilon(\lambda)$ obtained for different sections of the Deep River at Glendon (DR), Big Spring Creek at Big Spring (BSC), the Baraboo River at La Valle (BR), and the Wisconsin River at Muscoda (WR), which accounted to 5.78 m^{-1}, 2.73 m^{-1}, 29.26 m^{-1}, and 15.71 m^{-1}, respectively. We also determined the yellow substance light absorption at $\lambda = 440$ nm, which was as follows: for DR River – 4.44 m^{-1}, BSC – 0.41 m^{-1}, BR – 1.60 m^{-1}, and WR – 2.36 m^{-1}.

The calculation of the spectral contribution of the main optically active components of river water to spectral light attenuation, $\mathcal{E}(\lambda)$, at various sampling sites of the Ob River has shown that the yellow substance and suspension have the greatest optical influence on the total light attenuation. Here, the values of $\mathcal{E}(\lambda)$ and $\kappa_{ys}(\lambda)$ are given at the natural logarithmic base.

The largest contribution of yellow substance at $\lambda = 430$ nm was recorded in the surface layer of station 2.1 where it was 61.1%. At a wavelength of 550 nm, the yellow substance contribution varied from 21.3% (station 5.3) to 70.0% (station 3.2). At $\lambda = 670$ nm, the largest contribution of yellow substance was recorded at a depth of 5 m (station 3.2) and amounted to 39.4%.

Table. Light absorption by yellow substance (κ_{ys}), the concentration of yellow substance (C_{ys}) and chlorophyll *a* (*Chl*) at different stations of the Ob River

Station number	Depth, m	Coordinate	$\kappa_{ys}(450)$, m^{-1}	C_{ys}, $g \cdot m^{-3}$	*Chl*, $mg \cdot m^{-3}$
1.1	0	N 66°46'56,6» E 68°57'37,5»	4.0	18.8	17.0
1.2	2	N 66°46'56,6» E 68°57'37,5»	4.4	20.9	16.2
1.3	8	N 66°46'56,6» E 68°57'37,5»	4.4	20.7	22.6
2.1	0	N 66°46'49,5» E 68°57'35,3»	4.7	22.0	19.2
2.2	5	N 66°46'49,5» E 68°57'35,3»	4.7	22.4	20.5
2.3	20	N 66°46'49,5» E 68°57'35,3»	4.4	20.9	17.7
3.1	0	N 66°46'39,1» E 68°57'36,1»	4.5	21.2	17.9
3.2	5	N 66°46'39,1» E 68°57'36,1»	5.7	26.9	20.3
3.3	25	N 66°46'39,1» E 68°57'36,1»	5.0	23.6	16.5
4.1	0	N 66°46'32,6» E 68°57'24,4»	4.9	22.9	12.5
4.2	5	N 66°46'32,6» E 68°57'24,4»	4.8	22.8	21.6
4.3	20	N 66°46'32,6» E 68°57'24,4»	4.8	22.8	18.1
5.1	0	N 66°46'19,0» E 68°57'16,6»	4.6	21.7	20.2
5.3	14	N 66°46'19,0» E 68°57'16,6»	4.5	21.3	22.7

Suspension makes the largest contribution to the light attenuation at λ = 430 nm at station 2.3 and is just over 51%. The suspension contribution increases to 71.7% at the same station at λ = 550 nm. At the other stations, the suspension contribution was within a wide range from 26.3 to 74.7%. At λ = 670 nm, the suspension contribution at the Ob River varied from 22.8% (station 3.2) to 74.7% (station 2.3).

Pure water makes an insignificant contribution to the light attenuation at λ = 430 nm at all stations and is less than 0.1%. However, it increases sharply in the long-wave region where the values reach 20.7% at λ = 670 nm.

The contribution from chlorophyll at λ = 430 nm ranged from 8.3% (station 4.1) to 17.5% (station 1.3), while at λ = 550 nm, it varied from 1.6% (station 2.3) to 3.7% (station 1.3). At λ = 670 nm, the maximum chlorophyll contribution was observed at station 2.1, accounting for 36.5%.

Molecular light scattering by pure water in the investigated spectral range is responsible for a small contribution (0.1%).

Thus, for the Ob River waters, yellow substance and suspension appeared to be the most significant optically active components affecting the total light attenuation.

Chlorophyll *a* content at the Ob River site near the Salemal village was studied on August 27, 2020, at 14 stations and different layers (from the surface to 25 m). During the observation period, chlorophyll *a* concentration at different sites ranged from 12.5 to 22.7 mg·m^{-3} (Table). In our case, the maximum chlorophyll *a* concentration was recorded at a depth of 14 m (station 5.3) and amounted to 22.7 mg·m^{-3}. The amplitude and the maximum concentration of the main photosynthetic pigment of algae, chlorophyll, indicate that phytoplankton development at the Ob mouth at the end of August corresponds to highly eutrophic water bodies.

The development of phytoplankton in the Ob River at the end of August was high; in terms of its biomass, the water body in this period of the year can be classified as highly eutrophic according to I.S. Trifonova's trophicity scale (Trifonova, 1990), more than 10 g·m^{-3}. This also agrees with chlorophyll *a* content in the range from 12.5 to 22.7 g·m^{-3}.

4. Conclusions

New data were obtained on the optical characteristics of water at the mouth section of the Ob River during the period of the lowest water level and the maximum development of hydrobiocenoses. It was found that light attenuation ε(λ) in the spectral range from 400 to 800 nm varied widely from 1.5 to 21.5 m^{-1}; the index of light absorption by yellow substance $\kappa_{ys}(\lambda)$ was from 0.1 to 12.2 m^{-1}. The mean relative transparency measured with the Secchi disk at different stations was ~ 1.0 m. The concentrations of yellow substance in water samples ranged from 18.8 to 26.9 g·m^{-3} with an average value of 22.1 g·m^{-3}. New data on chlorophyll *a* content in the studied sites of the Ob river were obtained. The maximum content of chlorophyll *a* was recorded at a depth of 14 m and accounted for 22.7 mg·m^{-3}. It was found that the yellow substance and suspended solids were the most significant optically active components affecting the total light attenuation in the Ob River waters. The results obtained for the mouth of the Ob River agree with the data for other world rivers studied with the methodological approach based on the physical model of light attenuation in aquatic environments. This allows us to make recommendations for the inclusion of hydro-optical characteristics in the program of monitoring and forecasting the dynamics of aquatic ecosystems in the region under climate change and increasing anthropogenic load due to the use of natural resources.

Acknowledgments

The work was carried according to Agreement No. 3-2.4 / 2020 with the Non-Profit Partnership "Russian Center for Arctic Development" dated August 18, 2020, for conducting "Integrated research of the Gulf of the Ob within the framework of the "Environmental safety of the Ob-Irtysh River basin" project implementation in 2020", as well as within the framework of the state assignment for IWEP SB RAS (State registration of projects Nos AAAA-A17-117041210244-5 and AAAA-A17-117041210241-4).

Conflict of interests

The authors declare no conflict of interests.

References

Akulova O.B. 2015. Development of methods and a measuring computer system for assessing ecologically significant hydro-optical characteristics of freshwater reservoirs (by the example of lakes in Altai Krai). Cand. Sc. Dissertation, Institute for Water and Environmental Problems SB RAS, Barnaul, Russia. (in Russian)

Churilova T.Ya., Suslin V.V., Ryl'kova O.A. 2008. Parametrizatsiya pogloshcheniya sveta osnovnymi opticheski aktivnymi komponentami v Chernom more [Parameterization of light absorption by main optically active components in the Black sea]. Ekologicheskaya Bezopasnost' Pribrezhnoy i Shel'fovoy Zon i Kompleksnoe Ispol'zovanie Resursov Shel'fa [Environmental Safety of Coastal and Shelf Zones and Integrated Use of Shelf Resources] 16: 190-201. (in Russian)

Churilova T.Ya., Moiseeva N.A., Latushkin A.A. et al. 2018. Preliminary results of bio-optical investigations at Lake Baikal. Limnology and Freshwater Biology 1(1): 58-61. DOI: 10.31951/2658-3518-2018-A-1-58

Efimova V.T., Moiseeva N.A., Churilova T.Ya. et al. 2016. Pogloshchenie sveta opticheski aktivnymi komponentami sredy v zone fotosinteza glubokovodnoy chasti Chernogo morya (Sentyabr' 2015 goda) [Light absorption by optical active components of environment in the photosynthesis zone in the Black sea deep-water (September, 2015)]. Ekologicheskaya Bezopasnost' Pribrezhnoy i Shel'fovoy Zon Morya [Ecological Safety of Coastal and Shelf Zones of Sea] 4: 30-34. (in Russian)

Hong Y.U., Qiming C.A.I., Jinglu W.U. 2004. Study on optical properties of unpigmented suspended particles, yellow substance and phytoplankton algae in Taihu Lake. Chinese Journal of Oceanology and Limnology 22: 24-33. DOI: 10.1007/BF02842797

Julian J.P., Doyle M.W., Powers S.M. et al. 2008. Optical water quality in rivers. Water Resources Research 44. DOI: 10.1029/2007WR006457

Kopelevich O.V. 1983. Low-parametrical model of optical properties of seawater. In: Monin A.S. (Ed.), Optika okeana. T. 1. Fizicheskaya optika okeana [Ocean optics. Vol. 1. Physical optics of the ocean]. Moscow: Nauka, pp. 208-235. (in Russian)

Levin I.M. 2014. Few-parameter optical models of seawater inherent optical properties. Fundamental'naya i Prikladnaya Gidrofizika [Fundamental and Applied Hydrophysics] 7(3): 3-22. (in Russian)

Lobo F.L., Costa M.P.F., Novo E.M. et al. 2017. Effects of small-scale gold mining tailings on the underwater light field in the Tapajós River Basin, Brazilian Amazon. Remote Sensing 9. DOI: 10.3390/rs9080861

Man'kovsky V.I. 2011. Spectral contribution of the seawater components in the attenuation coefficient of directed light in the surface Mediterranean waters. Physical Oceanography 21(5): 305-319.

Man'kovsky V.I. 2015. Yellow substance in surface waters of the eastern part of the Tropical Atlantic. Physical Oceanography 3: 50-57. DOI: 10.22449/1573-160X-2015-3-50-57

Nyquist G. 1979. Investigation of some optical properties of seawater with special reference to lignin sulfonates and humic substances. PhD Thesis, Göteborg University, Sweden.

Pawlak B., Gąsowski R., Banaszak A. et al. 2003. Seasonal changes of light attenuation coefficient in selected points of the Oder River in the Szczecin Region, Poland. Polish Journal of Environmental Studies 12(2): 221-226.

Pope R.M., Fry E.S. 1997. Absorption spectrum (380–700 nm) of pure water. II. Integration cavity measurements. Applied Optics 36(33): 8710-8723. DOI: 10.1364/AO.36.008710

Shifrin K.S. 1983. Vvedenie v optiku okeana [Introduction to ocean optics]. Leningrad: Gidrometeoizdat. (in Russian)

Smith R.C., Baker K.S. 1981. Optical properties of the clearest natural waters (200–800 nm). Applied Optics 20(2): 177-184. DOI: 10.1364/AO.20.000177

Trifonova I.S. 1990. Ekologiya i suktsessiya ozernogo fitoplanktona [Ecology and succession of lake phytoplankton]. Leningrad: Nauka. (in Russian)

Yermolaeva N., Dvurechenskaya S., Kirillov V. et al. 2021. Dependence of long-term dynamics of zooplankton in the Ob River on interannual changes in hydrological and hydrochemical parameters. Water 13(14). DOI: 10.3390/w13141910

Limnology and Freshwater Biology 2021 (3): 1152-1155 DOI:10.31951/2658-3518-2021-A-3-1152

Short communication

ISSN 2658-3518
LIMNOLOGY FRESHWATER BIOLOGY
www.limnolfwbiol.com

Length-weight relationship and condition factor of endemic genus *Seminemacheilus* (Teloestei=Nemacheilidae) for Turkey

Seçer B.[1]*, Sungur S.[2], Çiçek E.[1], Mouludi-Saleh A.[3], Eagderi S.[3]

[1] *Department of Biology, Faculty of Art and Science, Nevsehir Hacı Bektas Veli University, Nevsehir, Turkey.*
[2] *Vocational School of Health Services, Nevsehir Hacı Bektas Veli University, Nevsehir, Turkey.*
[3] *Department of Fisheries, Faculty of Natural Resources, University of Tehran, Karaj, Iran.*

ABSTRACT. This study was aimed to determine the length-weight relationships and Fulton's condition factors of the genus *Seminemacheilus* that is endemic for Turkey. The specimens were collected from 2017 to 2019 using an electrofishing device (SAMUS 1000MP). The total length and the total weight of the examined specimens ranged from 3.5 to 9.1 cm and from 0.31 to 7.52 g, respectively. Based on the results, the growth coefficient values *b* ranged from 2.56 (*S. ispartensis*) to 3.48 (*S. attalicus*). Also, the condition factor of the studied fishes ranged from 0.77 (*S. dursunavsari)* to 1.11 (*S. attalicus)*. This study represents the first reports of length-weight relationship data for *S. ahmeti, S. attalicus, S. dursunavşari, S. ekmekciae,* and *S. ispartensis* from Turkish inland waters and four new maximum total lengths for the *Seminemacheilus* species. The results of this study provide useful information for further fisheries management, fish population dynamic studies and comparisons in future studies.

Keywords: Central Anatolia, Seminemacheilus, population dynamic, positive allometric

Introduction

The genus *Seminemacheilus* has six valid species, all of which are endemic to Central Anatolia. Six species viz. *Seminemacheilus lendlii*, *S. ispartensis, S. ahmeti*, *S. dursunavsari*, *S. ekmekciae*, and *S. attalicus* were reported from Turkish inland waters (Erk'akan et al., 2007; Çiçek et al., 2015; 2020; Sunger et al., 2018; Çiçek, 2020; Yoğurtçuoğlu et al., 2020). The Seminemacheilids has no trading value, but it is important for the Anatolian inland water bodies in Turkey for ichthyofauna and biodiversity (Kottelat, 2012).

Length-weight relationship (*LWR*) studies are a pre-requisite for assessing population characteristics of fishes (Le Cren, 1951) and provide basic knowledge in fisheries biology such as understanding the life cycle, evaluation of fish stocks, ontogenetic changes and growth studies, and conservation (Tabatabaei et al., 2015; Keivany et al., 2016; Jafari-Patcan et al., 2018; Eagderi et al., 2019). Therefore, these data are necessary for the management and conservation of fish populations.

Condition factor (*K*) is computed from the relationship between weight and length of fish species, with the aim of describing the "condition" of that fish individual (Froese, 2006). It is assumed that the growth of fish in ideal conditions maintain an equilibrium in length and weight and is a useful index for monitoring feeding intensity, age and growth rate, and for assessing the status of the aquatic ecosystem of fishes (Zamani-Faradonbe et al., 2015; Radkhah and Eagderi, 2015).

Despite the ecological importance of freshwater fishes, information about the length-weight relationship parameters and condition factors are often limited. Although *LWR* of *S. lendlii* is determined, there is no knowledge about the other five species of *Seminemacheilus* (Erk'akan et al., 2013; Mangıt et al., 2017).

Therefore, this study aimed to determine the length-weight relationship and Fulton's condition factor for six species of the endemic genus *Seminemacheilus* inhabiting Turkish inland waters.

Materials and methods

A total of 287 specimens of the *Seminemacheilus* species were collected from 2017 to 2019 from Kizilirmak, Sakarya, Konya Closed, and Mediterranean basins using an electrofishing device (Samus 1000) (Table 1; Fig. 1). After anesthesia, the specimens were fixed in 10% buffered formalin and transferred to the laboratory. The total length (*TL*) and the total

*Corresponding author.
E-mail address: buraksecer50@gmail.com (Seçer B.)

Received: August 13, 2021; ***Accepted:*** September 8, 2021;
Available online: October 05, 2021

weight of each individual were measured using digital calipers to the nearest 0.01 cm and 0.01 g, respectively. The length-weight relationship was determined by the method of least squares using the equation $W = a(TL)^b$ and logarithmically transformed into $\log(W) = \log(a) + b\log(TL)$ (Froese, 2006), where W is the whole-body weight (g); TL is the total length (cm); a is the intercept, and b is the slope. Prior to regression analyses, log-log plots of the length-weight pairs were performed to identify outliers (Froese et al., 2011). Outliers perceived in the log-log plots of all species were evacuated from the regression. The degree of correlation between the variables was assessed by the determination coefficient r^2. The significance level of r^2 was estimated by ANOVA. The student's t-test (ts) was used to determine whether parameter b is significantly different from the expected or theoretical value of 3 (i.e. $b = 3$, $P < 0.05$). All statistical analyses were performed in Excel 2016 and PAST v3.26. The condition factor (K) was determined by using the formula of $K = (W \times 100) / (TL)^3$, where TL is the total length (cm) and W is the whole-body weight of fish (g) (Fulton, 1904; Froese, 2006).

Results and discussion

The present study provides the LWRs data of six *Seminemacheilus* species, five of which have been determined for the first time. Moreover, based on our collected specimens, new maximum total lengths were recorded for four species, including *Seminemacheilus ahmeti* (7.5), *S. dursunavsari* (9.1), *S. ekmekciae* (8.2), and *S. ispartensis* (8.6). Table 2 provides the number of individuals, size range (*TL* (cm) and *W* (g)) and Fulton's Condition Factor. Regression parameters *a* and *b*, the 95% confidence limits of *b*, the 95% confidence limits of *a*, determination coefficient (r^2), and the type of growth for the studied species are given in Table 3.

The parameter *b* of the studied fishes ranged from 2.56 for *S. lendlii* to 3.48 for *S. attalicus*. It was reported that the value of *b* is generally between 2.5 and 4.0 (Tesch, 1971), though the ideal value of *b* is 3.0 (Froese, 2006). In this study, the *b*-values of the studied fish species are in the expected range. In a length-weight relationship, *b*-values that are higher and lower than 3 indicated positive and negative allometry, respectively. Based on the results, the growth pattern was positively allometric for *S. ahmeti*, *S. attalicus* and *S. ekmekciae*, isometric for *S. dursunavsari* and negatively allometric for *S. ispartensis* and *S. lendlii*.

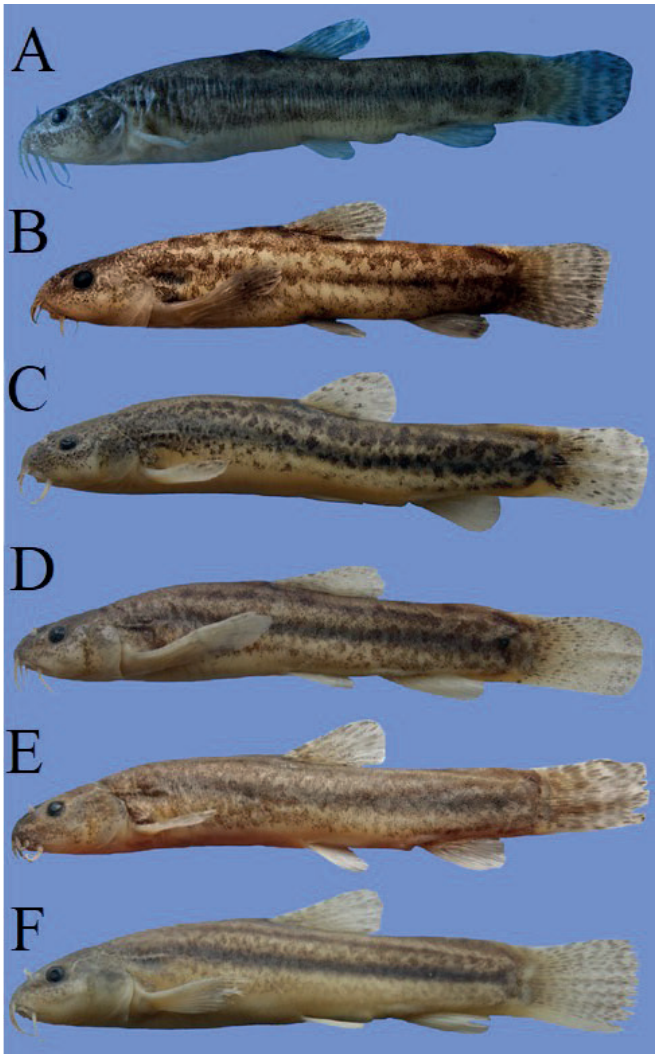

Fig.1. A - *Seminemacheilus ahmeti*, 49.7 mm standard length; B - *Seminemacheilus attalicus*, 55.5 mm standard length; C - *Seminemacheilus dursunavsari*, 57.3 mm standard length; D - *Seminemacheilus ekmekciae*, 53.4 mm standard length; E - *Seminemacheilus ispartensis*, 55.9 mm standard length; F - *Seminemacheilus lendlii*, 49.6 mm standard length.

The determination coefficient (r^2) between length and weight varied from 0.966 for *S. lendlii* to 0.988 for *S. attalicus*. The correlation coefficient (r) indicated a positive relationship between the length and weight of the studied species.

The values of condition factors (K) of the studied species ranged from 0.77 (*S. lendlii*) to 1.11 (*S.*

Table 1. Sampling stations data.

Species	Province	Habitat	Basin	Latitude	Longitude
S. ahmeti	Kayseri	Sultan Marsh	Kızılırmak	38°12'05"N	35°13'19"E
S. attalicus	Antalya	Kırkgöz wetland	Mediterranean	37°05'59"N	30°32'53"E
S. dursunavsari	Konya	Input of Alanözü pond	Eastern Mediterranean	37°07'48"N	32°42'19"E
S. ekmekciae	Konya	20 km nearest to Kulu	Konya Closed	39°02'13"N	32°48'36"E
S. ispartensis	Isparta	Isparta Creek	Mediterranean	37°52'22"N	30°46'47"E
S. lendlii	Afyonkarahisar	Spring canals at Hacıbeyli village	Sakarya	39°03'20"N	30°16'49"E

Table 2. Descriptive statistics for length and weight and Fulton's Condition Factor (*K*) for six species.

		TL(cm)		*W* (g)		Mean *K* (Range)
Species	**N**	**Min**	**Max**	**Min**	**Max**	
*Seminemacheilus ahmeti**	125	3.3	7.5	0.31	4.76	1.03 ± 0.11 (0.77-1.32)
*Seminemacheilus attalicus**	35	4.0	7.9	0.55	5.65	1.11 ± 0.10 (0.77-1.27)
*Seminemacheilus dursunavsari**	32	4.0	9.1	0.55	7.52	0.77 ± 0.08 (0.99-1.13)
*Seminemacheilus ekmekciae**	65	4.3	8.2	0.66	5.96	0.99 ± 0.11 (0.80-1.21)
*Seminemacheilus ispartensis**	15	4.2	8.6	0.78	5.35	1.02 ± 0.09 (0.84-1.20)
Seminemacheilus lendlii	15	4.2	7.7	0.78	3.82	0.99 ± 0.11 (0.84-1.20)

N - number of individuals; Min - minimum; Max - maximum; *K* - Fulton's Condition Factor
* first listing species

attalicus). Condition factor is an index that reflects the interactions between biotic and abiotic factors on the physiological state of fish; therefore, it is widely used to assess the state of the aquatic ecosystem, in which fish live. (Anene, 2005).

Conclusions

Seminemacheilus is the endemic genus to Central and Southwestern Anatolia of Turkey. This genus inhabits small streams and shallow ponds with sandy and clay bottoms covered by dense vegetation. All these species now live in very small habitats as the wetland has been drained and dried due to drought and habitat destruction in recent years.

This genus needs protection due to various ecological disturbances in its habitats. However, there is insufficient information about its biological properties. This study provides the first baseline data on the length-weight relationship and condition factor for the genus *Seminemacheilus*.

Conflict of interests

The authors declare no conflict of interests.

References

Anene A. 2005. Condition factor of four Cichlid species of a man-made lake in Imo State, Southeastern Nigeria. Turkish Journal of Fisheries and Aquatic Sciences 5: 43-47.

Çiçek E. 2020. *Seminemacheilus dursunavsari*, a new nemachelid species (Teleostei: Nemacheilidae) from Turkey. Iranian Journal of Ichthyology 7(1): 68-77. DOI: 10.22034/iji.v7i1.494

Çiçek E., Birecikligil S.S., Fricke R. 2015. Freshwater fishes of Turkey; a revised and updated annotated checklist. Biharean Biologists 9(2): 141-157.

Çiçek E., Sungur S., Fricke R. 2020. Freshwater lampreys and fishes of Turkey; a revised and updated annotated checklist 2020. Zootaxa 4809 (2): 241-270. DOI: 10.11646/zootaxa.4809.2.2

Eagderi S., Mouludi-Saleh A., Çiçek E. 2019. Length-weight relationship of ten species of Leuciscinae sub-family (Cyprinidae) from Iranian inland waters. International Aquatic Research 12: 133-136.

Erk'akan F., Nalbant T.T., Özeren S.C. 2007. Seven new species of *Barbatula*, three new species of *Schistura* and a new species of *Seminemacheilus* (Ostariophysi: Balitoridae: Nemacheilinae) from Turkey. Journal of Fisheries International 2(1): 69-85.

Table 3. Estimated parameters of length-weight relations and type of growth for six species.

		Regression parameters			95% CL of *a*	95% CL of *b*	GT
Species	**N**	***a***	***b***	**r^2**			
*S. ahmeti**	125	0.0063	3.28	0.970	0.0050-0.0078	3.16-3.40	+A
*S. attalicus**	35	0.0045	3.48	0.988	0.0028-0.0062	3.31-3.73	+A
*S. dursunavsari**	32	0.0078	3.12	0.984	0.0046-0.0105	2.97-3.39	I
*S. ekmekciae**	65	0.0057	3.30	0.969	0.0044-0.0071	3.18-3.44	+A
*S. ispartensis**	15	0.0187	2.62	0.985	0.0109-0.0252	2.44-2.95	-A
S. lendlii	15	0.0208	2.56	0.966	0.0134-0.0329	2.29-2.80	-A

N - number of individuals; GT - type of growth; *a* - intercept; *b* - slope; CL - confidence limits; r^2 - determination coefficient.
* first listing species

Erk'akan F., Innal D., Özdemir F. 2013. Length–weight relationships for ten endemic fish species of Anatolia. Journal of Applied Ichthyology 29: 683-684. DOI: 10.1111/jai.12140

Froese R. 2006. Cube law, condition factor and weight length relationships: history, meta-analysis and recommendations. Journal of Applied Ichthyology 22: 241-253. DOI: 10.1111/j.1439-0426.2006.00805.x

Froese R., Tsikliras A.C., Stergiou K.I. 2011. Editorial note on weight–length relations of fishes. Acta Ichthyologica et Piscatoria 30(10): 14-11. DOI: 10.3750/AIP2011.41.4.01

Fulton T.W. 1904. The rate of growth of fishes. 22nd Annual Report of the Fishery Board of Scotland 1904 (3): 141-241.

Jafari-Patcan A., Eagderi S., Mouludi-Saleh A. 2018. Length-weight relationship for four fish species from the Oman Sea, Iran. International Journal of Aquatic Biology 6(5): 294-295. DOI: 10.22034/ijab.v6i5.562

Keivany Y., Nezamoleslami A., Dorafshan S. et al. 2016. Length-weight and length-length relationships in populations of *Garra rufa* from different rivers and basins of Iran. International Journal of Aquatic Biology 3(6): 409-413. DOI: 10.22034/ijab.v3i6.6

Kottelat M. 2012. *Conspectus cobitidum*: an inventory of the loaches of the world (Teleostei: Cypriniformes: Cobitoidei). The Raffles Bulletin of Zoology Suppl. 26: 1-199.

Le Cren C.D. 1951. The length-weight relationship and seasonal cycle in gonad weight and condition in Perch, *Perca fluviatilis*. Journal of Animal Ecology 20: 201-219. DOI: 10.2307/1540

Mangıt F., Korkmaz M., Sü U. et al. 2017. Actual status of Eber Lake in terms of fish community structure. Journal of Limnology and Freshwater Fisheries Research 3(2): 101-106. DOI: 10.17216/LimnoFish.327824

Radkhah A., Eagderi S. 2015. Length-weight relationship and condition factor of Mosquitofish (*Gambusia holbrooki*) in three inland basins of Iran. Poeciliid Research 5(1): 39-43.

Sungur S., Jalili P., Eagderi S. et al. 2018. *Seminemacheilus ahmeti*, a new species of Nemachelid from Sultan Marshes, Turkey. Fishtaxa 3(2): 466-473.

Tabatabaei S.N., Hashemzadeh Segherloo I., Eagderi S. et al. 2015. Length-weight relationships of fish species in Kordan River (Namak Lake basin), Iran. Journal of Applied Ichthyology 31(4): 800-801. DOI: 10.1111/jai.12755

Tesch F.W. 1971. Age and growth. In: Ricker W.E. (Ed.), Methods for assessment of fish production in fresh waters. Oxford: Blackwell Scientific Publications, pp. 98-130.

Yoğurtçuoğlu B., Kaya C., Geiger M. 2020. Revision of the genus *Seminemacheilus*, with the description of three new species (Teleostei: Nemacheilidae). Zootaxa 4802(3): 477-501. DOI: 10.11646/zootaxa.4802.3.5

Zamani-Faradonbe M., Eagderi S., Shahbazi-Naserabad S. 2015. Length-weight relationships and condition factor of three fish species from Taleghan River (Alborz Province, Iran). Journal of Advanced Botany and Zoology 2(3): 1-3.